Journal of Bacteriology

Perturbation of FliL Interferes with Proteus mirabilis Swarmer Cell Gene Expression and Differentiation

Kathleen Cusick, Yi-Ying Lee, Brian Youchak and Robert Belas

Updated information and services can be found at:
http://jb.asm.org/content/194/2/437

These include:

SUPPLEMENTAL MATERIAL

http://jb.asm.org/content/suppl/2011/12/19/194.2.437.DC1.html

REFERENCES

This article cites 59 articles, 27 of which can be accessed free
at: http://jb.asm.org/content/194/2/437#ref-list-1

CONTENT ALERTS

Receive: RSS Feeds, eTOCs, free email alerts (when new
articles cite this article), more»

Information about commercial reprint orders: **http://jb.asm.org/site/misc/reprints.xhtml**
To subscribe to to another ASM Journal go to: **http://journals.asm.org/site/subscriptions/**

Journals.ASM.org

Perturbation of FliL Interferes with *Proteus mirabilis* Swarmer Cell Gene Expression and Differentiation

Kathleen Cusick,[a] Yi-Ying Lee,[b] Brian Youchak,[b] and Robert Belas[b]

Department of Microbiology, The University of Tennessee, Knoxville, Tennessee, USA,[a] and Department of Marine Biotechnology, University of Maryland Baltimore County, and Institute of Marine and Environmental Technology, Baltimore, Maryland, USA[b]

Proteus mirabilis is a dimorphic, motile bacterium often associated with urinary tract infections. Colonization of urinary tract surfaces is aided by swarmer cell differentiation, which is initiated by inhibition of flagellar rotation when the bacteria first contact a surface. Mutations in *fliL*, encoding a flagellar structural protein with an enigmatic function, result in the inappropriate production of differentiated swarmer cells, called pseudoswarmer cells, under noninducing conditions, indicating involvement of FliL in the surface sensing pathway. In the present study, we compared the *fliL* transcriptome with that of wild-type swarmer cells and showed that nearly all genes associated with motility (flagellar class II and III genes) and chemotaxis are repressed. In contrast, spontaneous motile revertants of *fliL* cells that regained motility yet produced differentiated swarmer cells under noninducing conditions transcribed flagellar class II promoters at consistent levels. Expression of *umoA* (a known regulator of swarmer cells), *flgF*, and *flgI* increased significantly in both swarmer and pseudoswarmer cells, as did genes in a degenerate prophage region situated immediately adjacent to the Rcs phosphorelay system. Unlike swarmer cells, pseudoswarmers displayed increased activity, rather than transcription, of the flagellar master regulatory protein, FlhD$_4$C$_2$, and analyses of the *fliL* parent strain and its motile revertants showed that they result from mutations altering the C-terminal 14 amino acids of FliL. Collectively, the data suggest a functional role for the C terminus of FliL in surface sensing and implicate UmoA as part of the signal relay leading to the master flagellar regulator FlhD$_4$C$_2$, which ultimately controls swarmer cell differentiation.

Proteus mirabilis is an enterobacterial opportunistic urinary tract pathogen that causes infections often associated with indwelling catheters or structural abnormalities of the urinary tract (reviewed in references 19 and 39). These infections are aided by several virulence factors, with one of the most significant being the ability of these bacteria to respond to the surfaces of host cells in a behavior referred to as swarming that allows *P. mirabilis* to move from an initial site of colonization (for example, a catheter surface) to uroepithelial cells of the urinary tract (3, 30, 41).

Swarming is a flagellum-dependent motile behavior that is distinct from swimming in that it is a multicellular process that occurs on solid surfaces or in viscous liquids. Swarming behavior requires differentiation of vegetative swimmer cells into highly elongated, hyperflagellated swarmer cells (4, 31). Swarmer cell differentiation is initiated upon contact with a solid surface, which inhibits flagellar rotation, and an obligate requirement exists for this stimulus, as swarmer cells removed from a surface quickly dedifferentiated to vegetative swimmer cells (1, 23, 47, 52). Other conditions that inhibit flagellar rotation, such as addition of compounds that increase fluid viscosity or antisera to FlaA (flagellin structural protein of the flagellar filament) to liquid media, induce swarmer cell differentiation and transcription of swarmer cell genes (16). The importance of the flagellum as an integral component of the surface-sensing mechanism is underscored by several reports showing that mutations in many different flagellar genes results in an inability of *P. mirabilis* to differentiate (12, 14, 24, 26).

The bacterial flagellum is comprised of three main substructures—the basal body, the hook, and the helical filament—and the synthesis of each is coordinated by a finely regulated regulatory circuit (38). In *Escherichia coli*, *Salmonella enterica* serovar Typhimurium, and *P. mirabilis*, regulation of flagellar biosynthesis occurs as a three-level regulatory cascade involving class I, class II,

and class III transcriptional promoters (32, 33). The sole class I promoter controls expression of the *flhDC* operon, encoding the flagellar master regulator, which in turn activates transcription of the class II operons. Class II promoters control genes encoding the export apparatus, basal body and hook proteins, and regulatory proteins that control transcription of class III operons. Class III promoters transcribe *flaA* (flagellin) and late genes required for filament assembly, motility, and chemotaxis. The activity of FlhDC is controlled in multiple ways. In *P. mirabilis*, these means of control include the RcsCDB phosphorelay system, which is activated upon growth on a surface (22), and four proteins, UmoA, UmoB, UmoC, and UmoD, that were discovered during a search for upregulators of the master operon (20).

While the role of most of the proteins comprising the flagellum is understood, the function of one, FliL, remains enigmatic. FliL is a small protein—*P. mirabilis* FliL is 18.2 kDa—found in many flagellated bacterial species. FliL homologs are located in the inner membrane and have a single transmembrane domain (which in *P. mirabilis* is located near the N terminus ca. 10 residues from the start), such that the N terminus of the protein resides in the cytoplasm and the C terminus in the periplasm (11). In *P. mirabilis* and many other species, *fliL* is the lead gene in a class II flagellar operon (*fliLMNOPQR*). Despite its ubiquity, the FliL sequence is poorly

conserved between species, with only 51% identity shared between *P. mirabilis* FliL and FliL of *E. coli* or *S.* Typhimurium.

FliL has been thought to be a nonessential component of the basal body, since it is not required for swimming by either *S.* Typhimurium or *E. coli* (45); however, *S.* Typhimurium does not swarm when *fliL* is mutated (11). Attmannspacher et al. discovered that Δ*fliL* strains lose their flagella more readily than the wild type, with the dislodged flagella ending in a hook and partial rod structure that results from breaks between the proximal (FlgF) and distal (FlgG) rod proteins (11). Breakage of the flagella occurs only with functioning motors and is independent of the direction of filament rotation, leading to the conclusion that *S.* Typhimurium FliL is likely part of the motor stator (MotA and MotB), where it strengthens and stabilizes rod attachment, a function that is especially important as torque develops on the flagella during swarming on an agar surface (11).

We previously reported on a *P. mirabilis fliL* strain (BB2204; *fliL*₂₂₀₄::Tn5-CM) that is nonmotile, i.e., it does not swim or swarm, and that inappropriately produces elongated swarmer cells in both broth and agar (16). This mutation causes polar effects on essential downstream genes in the *fliL* operon, resulting in the nonmotile phenotype. Supporting this idea, Western blots with anti-FlaA antisera showed that BB2204 does not produce flagellin (16). However, polar effects alone cannot explain the presence of swarmer cells in broth-grown *fliL* strains, since independent mutations in other genes within the *fliL* operon (*fliM*, *fliP*, and *fliQ*) result in cells that never differentiate under any condition (16). Mutations in *fliL* not only result in the production of swarmer cells under noninducing conditions (referred to as "pseudoswarmer" cells to distinguish them from differentiated swarmer cells resulting from contact with a surface) but also result in increased expression of two swarmer cell-dependent genes, *zapA* and *hpmBA* (16). Thus, FliL, a hook–basal-body-associated protein, appears to be a critical component of the *P. mirabilis* surface signal sensory transduction pathway that controls transcription of swarmer cell genes.

In the present study, we sought further understanding of the molecular mechanisms underlying the ability of *P. mirabilis* to sense a surface. Global transcriptional profiling of genes expressed in three cell types, wild-type swimmer cells, wild-type swarmer cells, and *fliL* pseudoswarmer cells, identified changes in expression, and this analysis was complemented by a study of a set of stable, spontaneous motile revertants from the *fliL* parent strain. We discovered that (i) while both swarmer and pseudoswarmer cells increased expression of many genes, similar patterns of regulation were shared in only a few, most notably *umoA*, *flgF*, and *flgI*, and genes encompassing a degenerate prophage region adjacent to the *rcs* genes; (ii) *fliL* pseudoswarmer cells displayed increased activity rather than transcription of the flagellar master regulatory protein, FlhD₄C₂, and (iii) both pseudoswarmers and motile revertants contained mutations that altered the C-terminal 14 amino acids of FliL. Our combined transcriptomic and genetic analyses indicate that the C terminus of FliL plays an important role in the pseudoswarmer phenotype.

MATERIALS AND METHODS

Strains, culture conditions, and media. *P. mirabilis* BB2000 served as the wild type and parent of BB2204 (16), which is a FliL⁻ mutant resulting from insertion of Tn5-Cm in *fliL* (Table 1). Strains were maintained in Luria-Bertani (LB) broth (Bacto tryptone, 10 g liter⁻¹; yeast extract, 5 g

TABLE 1 Strains and primers

Strain or primer	Characteristics/sequence	Reference or source
P. mirabilis strains		
BB2000	Wild type; spontaneous Rfʳ from PRM1	13
BB2204	BB2000 *fliL*::Tn5-Cm	16
YL1001	Motile revertant of BB2204; Cmˢ	This study
Primers		
fliLpF	GGATCCGTGGTGTCGATATTT	
fliL_r	GAGCATCTATCTCTGCCTGTGAAAGG	
rpoAF	GCGTGTTATAGCCCAGTTGA	
rpoAR	AGGCTGACGAACATCACGTA	
flhDF	AAGGCTTCCGCAATGTTTAGAC	
flhDR	GTTGCAAATCATCCACTCTGGA	
fliAF	CCTGCGAGTGTTGAATTGGA	
fliAR	GGATTGTGTCACTTCTCTTGC	
fliLF	GGTGATCGCCATTATTGCAG	
fliLR	AGCGTAACGTGATCCCTATG	
fliMF	GTCAATTCCGTATGGGGCTG	
fliMR	AACCAGATTCGGCTCAAAGG	
flgMF	CGCACAAATCCACTTATCCC	
flgMR	GGGCAACTTTTTCGACATTG	
flaAF	CAACTGAAGGTGCATTGAAC	
flaAR	TGATTTCTCACCGCTCAGTA	
motAF	GATGGTGACGGGGAATATGAA	
motAR	CCATTTCCCCAGCAGGTCTA	
umoAF	TCCACCACCACCACACGTAA	
umoAR	CGCAATCCTTTGCCTGTCCTA	
umoBF	TATATGCCTCCAAACCTTTCCA	
umoBR	AGCTTGGGTTTACACGGTTG	
umoCF2	CTCTTTTTCCTCCTTTGCTCA	
umoCR2	CACTATCTTCAAGGTCGCCT	
umoDF	CAAGAGTGCCGTGTTTTCTATA	
umoDR	CGATGATATCGCCCGGTTTAA	
wosAF2	GCCCCTTATGCTGTCATGAA	
wosAR2	GCCATTCAAAATCTGGTCACG	
rcsFF	CTCCTGTTCGCATTGTTGAA	
rcsFR	TTCCTGTGACTATTTGGCATTC	
rsbAF	CTATACCTACCGCACCATGT	
rsbAR	GAAGTCCCATCCGTTGATAC	
rcsBF	CGCCTGCTGATCTACCTAAA	
rcsBR	GCAATCTCAGTGACAAGGAA	
rcsCF	CGGCTACCCACATTTTCTTGA	
rcsCR	CCGGCAGAGGGATAAATGAAA	
mrpAF	TGATGCTCCTTGCTCAATTAC	
mrpAR	AGTTGCTTCAGAGCCAGTGA	
ucaJF	GGAGGGAAATAGCCCATTCA	
ucaJR	TTGGCATAATGCTTTCTGCTGA	
pmpJF	CTTGATGTGAGTCAGCAACA	
pmpJR	CACGCAAATAGAATGGAAACG	
hpmBF	GGCGTTGAATGGCTAAGTTTA	
hmpBR	CCACCTTGCCATCCTTTGTA	
zapAF	GGCCAAGCATGGTTTAGTGA	
zapAR	GGCGACTATCTTCCGCATAA	

liter⁻¹; sodium chloride, 10 g liter⁻¹) (50) or LB agar (LB containing 15 g liter⁻¹ Bacto agar) at 37°C. When isolated colonies were required, LSW⁻ agar (Bacto tryptone, 10 g liter⁻¹; yeast extract, 5 g liter⁻¹; NaCl, 0.4 g liter⁻¹; glycerol, 5 ml liter⁻¹; Bacto agar, 20 g liter⁻¹) (13) was used to prevent swarming in Swr⁺ strains. Swimming motility was determined in Mot agar (Bacto tryptone, 10 g liter⁻¹; NaCl, 5 g liter⁻¹; Bacto agar, 3 g liter⁻¹). Chloramphenicol (40 µg ml⁻¹) was used to maintain Tn5-Cm in BB2204.

Phenotypic analysis of mutants. Spontaneous motile revertants of BB2204 were obtained after incubation on LB agar or in Mot agar, as follows: 5 μl of an overnight culture was placed in the center of an LB agar plate to detect swarming motility, while 30 μl of an overnight culture was inoculated into the diameter across a Mot agar plate to detect swimming motility. Bacteria were incubated at 37°C until motile flares appeared, at ca. 3 to 5 days. Swimming of the motile revertants was determined by measuring the migration of the cells through semisolid Mot agar. Aliquots (5 μl each) from overnight cultures grown in Mot broth (Mot agar less agar) were inoculated into Mot agar, and the bacteria were incubated in a moisture chamber. Swarming motility was assessed as the cells migrated over the surface of LB agar. Overnight cultures grown in LB broth were diluted to an optical density at 600 nm (OD_{600}) of 0.4 in 1× phosphate-buffered saline (PBS; 8 g liter^{-1} NaCl, 0.2 g liter^{-1} KCl, 1.44 g liter^{-1} Na$_2$HPO$_4$, 0.24 g liter^{-1} KH$_2$PO$_4$), and 5-μl aliquots were spotted onto LB agar and incubated with a constant humidity of 46%.

For both swimming and swarming revertants, swarmer cell differentiation (i.e., cellular elongation to lengths typical of wild-type cells obtained from agar) in liquid media was measured using phase-contrast light microscopy (Olympus BX60) and compared with that of broth-grown wild-type (BB2000) and pseudoswarmer (BB2204) cells. All strains (BB2000, BB2204, and revertants) were grown overnight in LB broth, inoculated into fresh LB at a 1:100 dilution, and incubated at 37°C with shaking (200 rpm). Cell length and morphology were examined every 30 min. Both mean cell length (± standard deviation) and the number of elongated cells in the population were determined. A cell was considered a differentiated swarmer cell if its cell length was >7 μm or >3-fold a "floating standard" of the mean cell length of wild-type cells (BB2000) grown in LB broth for the same incubation period.

Transcription and regulation of select flagellar genes and genes defined as essential to swarming were examined in revertants, and transcript levels were compared to those in broth-grown wild-type and *fliL* pseudoswarmers via reverse transcription-PCR (RT-PCR) and quantitative reverse transcriptase PCR (qRT-PCR). For expression analysis of revertants, cells were harvested from liquid cultures incubated at 37°C that displayed the greatest proportion of the pseudoswarmer phenotype—i.e., when populations of both BB2204 and YL1001 contained the greatest number of elongated cells (2.5 h of incubation, when the OD_{600} was approximately 0.9).

RNA sequencing sample collection and RNA extraction. An RNA sequencing (RNA-Seq) analysis was performed to identify the underlying molecular mechanisms contributing to the *fliL* phenotype. To provide a platform from which to compare the pseudoswarmer transcriptome, RNA-Seq was also performed on wild-type swarmer cells (i.e., BB2000 grown on agar). For transcriptomic analysis of pseudoswarmer cells, single colonies of BB2204 and BB2000 (serving as the control sample when determining levels of change in RNA-Seq analysis) were inoculated into 2 ml LB broth and incubated with agitation (200 rpm) at 37°C. Cells were harvested at 4.5 h, based on microscopic observations of *fliL* pseudoswarmer elongation. For transcriptomic analyses of wild-type swarmer cells, single colonies were grown overnight in 2 ml LB broth, followed by washing in LB broth. Swarmer cell samples were diluted in 1× PBS, and 100 μl of a 10^{-2} dilution was spread onto LB plates that had been dried for 30 min at 42°C prior to inoculation, while samples of swimmer cells, serving as the control for determining the levels of change (fold), were reinoculated into fresh LB broth at a 1:10 dilution. Both sample types were harvested 4.3 h after inoculation, with swarmer cells collected using the method of Wang et al. (57). Cultures were pelleted at 10,000 × *g* for 5 min at room temperature, washed with 1× PBS, and repelleted. The cell pellets were snap-frozen in a dry-ice–ethanol slurry and stored in RNase-free tubes at −80°C prior to RNA extraction.

RNA extraction. Total RNA from all samples was extracted using a Ribopure kit (Ambion) following the manufacturer's instructions, with the DNase treatment extended to 1 h. The RNA concentration and purity of each sample were measured using a Nano-drop 1000 spectrophotom-eter (Thermo Scientific). An mRNA enrichment step was performed on samples designated for RNA-Seq using a MICROBExpress kit (Ambion) in order to reduce sequencing of 16S and 23S rRNA. The degree of rRNA depletion was evaluated with an mRNA assay, using an Agilent 2100 Bioanalyzer with a RNA 6000 Nano LabChip kit (Agilent).

cDNA synthesis, RT-PCR, and quantitative RT-PCR. For all samples but aliquots designated for RNA-Seq, 1 μg total RNA was reverse-transcribed into cDNA using a high-capacity cDNA reverse transcription kit with RNase inhibitor (Applied Biosystems). Thermocycling conditions were as follows: 25°C for 10 min, 37°C for 2 h, 85°C for 5 min. For RT-PCRs, each reaction mixture (50 μl) contained 1× ThermoPol buffer, 25 ng cDNA, a 200 nM concentration of each primer, 200 μM deoxynucleoside triphosphates (dNTPs), and 5 U *Taq* polymerase (NEB). Thermocycling conditions were as follows: 94°C for 3 min; 30 cycles of 94°C for 1 min, 60°C for 30 s, and 72°C for 20 s; and 72°C for 2 min. qRT-PCR was performed with the 2× Power SYBR green kit (Applied Biosystems). Reaction mixtures consisted of 2× SYBR green master mix, a 100 to 300 nM concentration of each forward and reverse primer, and 25 ng cDNA template, and each was brought to a final volume of 25 μl with nuclease-free water. Reactions were performed on the ABI 7500 fast real-time PCR system using the following protocol: 50°C for 2 min, 95°C for 10 min, followed by 40 cycles of 95°C for 15 s and 60°C for 1 min. A dissociation curve analysis was performed for each assay to ensure product specificity (95°C for 15 s, 60°C for 1 min, 95°C for 15 s). The sequences for all primers are listed in Table 1. The amount of change (fold) was calculated using the $2^{-\Delta\Delta CT}$ formula (37), with *rpoA* serving as the housekeeping gene. In cases where the PCR efficiencies were not comparable between housekeeping and functional genes, change was calculated using the equation describe by Pfaffl (44). Serial dilutions spanning 5 orders of magnitude were used to calculate the slope of each assay, and PCR efficiency was then determined by the expression $10^{(-1/\text{slope})}$ (7). Several different genes were assessed for use as an appropriate reference gene, and under the conditions used in this study, *rpoA* expression remained unchanged (data not shown).

qRT-PCR was also used to validate the results of the RNA-Seq analysis. RNA was extracted from two independent cultures grown under the conditions described for RNA-Seq sample collection. Assays were run in triplicate on total RNA (i.e., prior to mRNA enrichment) and in duplicate on mRNA-enriched samples. Genes (*flhD*, *motA*, *flaA*, *umoA*, *zapA*, and *hpmB*) were selected based on a combination of the following criteria: (i) differential expression in RNA-Seq and (ii) applicability to both swarmer and *fliL* transcriptomes.

RNA-Seq. cDNA library preparation, sequencing, and preliminary bioinformatic analysis were performed at the University of Maryland, Baltimore's Institute for Genomic Sciences (IGS) following standard protocols. Briefly, cDNA libraries were prepared with an mRNA-Seq sample preparation kit (Illumina Inc., San Diego, CA) following a variation of the manufacturer's protocol. The DNA was purified between enzymatic reactions, and size selection of the library was performed with AMPure XT beads (Beckman Coulter Genomics, Danvers, MA). One sample per lane was loaded onto the flow cell and sequenced in 50-nucleotide paired-end runs on the Illumina genome analyzer II (GAII).

Primary image processing was done via the Illumina pipeline (which included Firecrest for image analysis, Bustard for base calling, and GERALD for alignment and visualization). The Phred-like quality scores (assigned to each base of each raw read via Bustard) were further analyzed via the IGS quality control pipeline. Values were plotted to evaluate per-cycle/base statistics, and any data falling below the minimum quality threshold were removed from the final data set. Raw reads were mapped to the *P. mirabilis* HI4320 reference genome with the Mosaik aligner (http://bioinformatics.bc.edu/marthlab/Mosaik), allowing for 2-nt mismatches. The genome of *P. mirabilis* HI4320 has been sequenced and published (43) and is nearly identical to that of BB2000, based on the current transcriptomic analysis. Therefore, nucleotide sequences derived from HI4320 were used for the RNA-Seq analysis of BB2000 and BB2204.

Raw reads were normalized to reads per kilobase of gene (exon) per million mapped reads (RPKM values) (40), using an IGS in-house pipeline built around a combination of Burrows-Wheeler Aligner (34) and TopHat/Cufflinks (54, 55).

Genes involved in swarmer cell differentiation were identified by comparing the transcriptomes of swarmer (i.e., agar-grown) versus swimmer (broth-grown) wild-type cells, while a comparison of the transcriptomes of *fliL* pseudoswarmers and wild-type swimmer cells was used to uncover genes expressed when FliL was defective. Additionally, the transcriptomes of *fliL* pseudoswarmers and wild-type swarmer cells were also compared. Statistical analyses were performed on raw reads of each sample set with DESeq, an R software package available on Bioconductor based on the negative binomial distribution (5). Thus, three sample sets were analyzed with DESeq: (i) wild-type swarmer versus swimmer cells, (ii) *fliL* pseudo-swarmer versus wild-type swimmer cells, and (iii) *fliL* pseudoswarmer versus wild-type swarmer cells. Sample change (fold) was calculated by dividing the normalized reads (RPKMs) for each sample set as follows: (i) swarmer/swimmer, (ii) *fliL* pseudoswarmer/wild-type swimmer, and (iii) *fliL* pseudoswarmer/swarmer. Genes with a change in expression (fold change ratio) of >2 or <0.5, with a statistical significance of a P value of <0.05, were considered significantly differentially expressed. In an effort to identify major biological themes associated with swarmer and *fliL* cell types, a Gene Ontology enrichment analysis was performed on each data set using GoMiner "omic data analysis" software (http://discover.nci.nih.gov/gominer/index.jsp) (60, 61). In this analysis, the enrichment factor is a relative measure based on the total number of differentially expressed genes in a particular category relative to the total number of genes in that category, normalized to the total number of differentially expressed genes in the transcriptome.

Nucleotide sequencing. The *fliL* gene from BB2000, BB2204, and 17 motile revertants was sequenced using an ABI3130 XL genetic analyzer at the BioAnalytical Services Lab (University of Maryland Institute of Marine and Environmental Technology, Baltimore, MD).

Nucleotide sequence accession numbers. The data discussed in this publication have been deposited in NCBI's Gene Expression Omnibus (21) and are accessible through GEO Series accession number GSE30810 (http://www.ncbi.nlm.nih.gov/geo/query/acc.cgi?acc=GSE30810).

RESULTS

Analysis of the wild-type swarmer cell transcriptome. RNA sequencing resulted in the following total reads for each sample: 35,306,504 from *fliL* pseudoswarmer cells, 19,885,858 from wild-type swimmer cells (for comparison with *fliL* pseudoswarmers), 21,920,064 from wild-type swarmer cells, and 24,950,582 from a second sample of wild-type swimmer cells, used for comparison with wild-type swarmer cells. The total reads for each sample, along with reads that mapped uniquely, unmapped reads, and reads that mapped to multiple locations, are summarized in Table S1 in the supplemental material. More than 96% of the reads for each sample mapped uniquely to the reference genome, while the remaining 4% either were unmappable or mapped to multiple locations.

As a foundation for comparisons to the *fliL* pseudoswarmer transcriptome, gene expression in wild-type swarmer cells was compared to that in wild-type swimmer cells, resulting in the identification of 185 significantly differentially expressed genes in the swarmer cell transcriptome. Approximately 27% (51 of 185) of these genes were associated with flagellar biosynthesis and regulation and/or chemotaxis proteins (Fig. 1; Table 2), a finding corroborated by GoMiner analyses, which showed significant enrichment of transcripts involved with flagellar motility ($P = 1.2 \times 10^{-35}$), flagellar assembly ($P = 3.6 \times 10^{-21}$), flagellar organization ($P = 1.3 \times 10^{-33}$), and chemotaxis ($P = 4.2 \times 10^{-19}$). In agreement with prior expression profiling of *P. mirabilis* swarmer
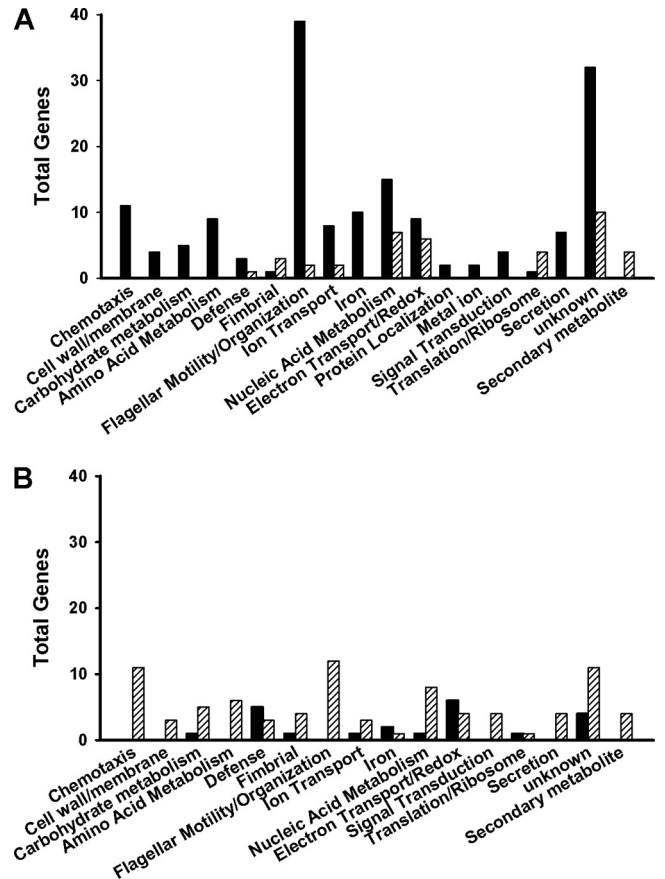
FIG 1 Functional categories of genes whose expression significantly increased (A) or decreased (B) in swarmer cells (black bars) or pseudoswarmer cells (hatched bars). Genes were grouped according to their Gene Ontology (GO) categories assigned by GoMiner. Putatively annotated genes for which no GO terms have yet been assigned were categorized based on their COG or Kyoto Encyclopedia of Genes and Genomes (KEGG) ontology pathway (6) designations.

cells (42), many of the 51 flagellar genes were highly induced. For example, the expression of *fliE* (secretion apparatus) and *fliA*, encoding σ^{28} subunit of RNA polymerase, increased 222- and 158-fold, respectively, while genes encoding the hook-basal body complex (i.e., *flgE*, *flgC*, and *flgB*) were all induced 160- to 190-fold (Table 2) (42).

Numerous genes whose products are involved with outer membrane fluidity, membrane permeability, and cell wall function also exhibited increased expression in swarmer cells (see Table S2 in the supplemental material). These included genes encoding multiple lipoproteins (PMI0993, PMI0994, PMI3460, PMI1840, PMI0743, and *nlpA* [PMI1318]), outer membrane proteins (PMI1359, PMI0842, PMI2950, and *ireA* [PMI1945]), a glycoporin (*rafY* [PMI0288]), a glycosyl hydrolase (PMI0290), and a β-phosphoglucomutase (*pgmB* [PMI0289]). *exbD* (PMI0030) and *exbB* (PMI0029), encoding biopolymer proteins postulated to transfer signals related to iron transport across the outer membrane (28), were also induced. A complete list of all significantly differentially expressed genes may be found in Table S2 in the supplemental material.

Analysis of the *fliL* pseudoswarmer cell transcriptome. When the transcriptome of *fliL* pseudoswarmer cells (BB2204) was com-

TABLE 2 The 50 most highly expressed genes in the wild-type *P. mirabilis* swarmer cell transcriptome ($P < 0.05$)[a]

Locus tag	Gene	Product	Fold change
PMI1629	*fliE*	Flagellar hook-basal body complex protein	222.21
PMI1651	*flgE*	Flagellar hook protein	188.70
PMI1653	*flgC*	Flagellar basal-body rod protein	183.85
PMI1630	*fliF*	Flagellar MS ring protein	176.34
PMI1654	*flgB*	Flagellar basal body rod protein	161.84
PMI1618	*fliA*	Flagellar biosynthesis sigma factor	157.71
PMI1961	*ccm*	Membrane protein	143.67
PMI1652	*flgD*	Basal-body rod modification protein	126.18
PMI0993	NA	Lipoprotein	123.58
PMI1649	*flgG*	Flagellar basal-body rod protein (distal rod protein)	106.70
PMI1631	*fliG*	Flagellar motor switch protein G	105.74
PMI1650	*flgF*	Flagellar basal-body rod protein	101.75
PMI1638	*fliN*	Flagellar motor switch protein	96.66
PMI1620	*flaA*	Flagellin 1	82.22
PMI0994	NA	Lipoprotein	75.58
PMI2808	NA	Methyl-accepting chemotaxis protein	72.94
PMI1634	*fliJ*	Flagellar biosynthesis chaperone	72.21
PMI1628	NA	Metalloelastase	71.00
PMI2834	*aad*	Amino acid deaminase	69.92
PMI1621	*fliD*	Flagellar capping protein	67.94
PMI0289	*pgmB*	β-Phosphoglucomutase	67.79
PMI0290	NA	Glycosyl hydrolase	60.48
PMI1635	*fliK*	Flagellar hook length control protein	56.15
PMI0288	*rafY*	Glycoporin	56.01
PMI1632	*fliH*	Flagellar assembly protein H	51.11
PMI1645	*flgK*	Flagellar hook-associated protein 1	51.07
PMI1648	*flgH*	Flagellar basal body L-ring protein	48.06
PMI1644	*flgL*	Flagellar hook-associated protein 3	40.45
PMI1617	*fliZ*	Flagellar biosynthesis protein	39.98
PMI1359	NA	Outer membrane protein	39.00
PMI1637	*fliM*	Flagellar motor switch protein	36.70
PMI1636	*fliL*	Flagellar basal body-associated protein	36.66
PMI2898	NA	Amino acid ABC transporter	34.56
PMI3460	NA	Lipoprotein	33.39
PMI1660	*flhB*	Flagellar biosynthesis protein	32.91
PMI1646	*flgJ*	Flagellar rod assembly protein	32.91
PMI0842	NA	Putative outer membrane receptor	32.32
PMI0833	NA	Hypothetical protein	32.27
PMI1647	*flgI*	Flagellar basal-body P-ring protein	30.94
PMI0992	NA	Hypothetical protein	29.00
PMI2149	NA	Exported amino acid deaminase	28.61
PMI0291	*treB*	PTS trehalose (maltose)-specific transporter	27.74
PMI1623	*fliT*	Flagellar protein	27.21
PMI1622	*fliS*	Flagellar protein	26.56
PMI1442	NA	Hypothetical protein	26.43
PMI1659	*flhA*	Flagellar biosynthesis protein	25.56
PMI1245	NA	Hypothetical protein	25.00
PMI0176	NA	Iron transport	24.07
PMI1662	*cheY*	Chemotaxis response regulator	23.76

[a] For all RNA-Seq analysis tables, P was <0.05, as determined via DESeq analysis. NA, not applicable; MS, membrane-supramembrane; PTS, phosphotransferase system.

TABLE 3 The 25 most highly induced and repressed genes in the transcriptome of *fliL* pseudoswarmer cells[a]

Locus tag	Gene	Product	Fold change
PMI2722	NA	Microcompartment protein	15.31
PMI2718	NA	Hypothetical protein	14.6
PMI2720	NA	Microcompartment protein	9.68
PMI2719	NA	Aldehyde-alcohol dehydrogenase	7.57
PMI2721	NA	Microcompartment protein	7.22
PMI0536	*uca*	Major fimbrial subunit	6.93
PMI1722	NA	Phage protein	5.42
PMI0534	NA	Fimbrial usher protein	4.7
PMI0535	NA	Fimbrial chaperone	3.97
PMI3091	NA	Fimbrial subunit	3.72
PMI1721	NA	Phage protein	3.7
PMI1250	NA	Transcriptional regulator	3.65
PMI1720	NA	Phage protein	3.43
PMI2987	NA	Hypothetical protein	3.22
PMI1180	NA	Methyl-accepting chemotaxis protein	3.21
PMI2399	*tetAJ*	Tetracycline resistance protein	3.02
PMI1647	*flgI*	Flagellar basal body P-ring protein	2.97
PMI1650	*flgF*	Flagellar basal-body rod protein	2.9
PMI1710	NA	Phage protein	2.8
PMI1025	*sitC*	Iron ABC transporter, membrane protein	2.69
PMI1719	NA	Phage protein	2.63
PMI2916	NA	Acetyltransferase	2.58
PMI0068	NA	Hypothetical protein	2.5
PMI2716	NA	Propanediol utilization protein	2.45
PMI1712	NA	Phage protein	2.35
PMI3003	NA	Fimbrial operon regulator	0.16
PMI1468	NA	Fimbrial subunit	0.16
PMI2908	NA	β-Ketoacyl-ACP synthase	0.15
PMI0578	NA	MFS-family transporter	0.15
PMI2030	NA	Toxin transporter	0.15
PMI1637	*fliM*	Flagellar motor switch protein FliM	0.15
PMI1644	*flgL*	Flagellar hook-associated protein 3	0.14
PMI1662	*cheY*	Chemotaxis response regulator	0.13
PMI1661	*cheZ*	Chemotaxis regulator CheZ	0.1
PMI1663	*cheB*	Chemotaxis response regulator protein	0.09
PMI1622	*fliS*	Flagellar protein FliS	0.09
PMI2813	*aer*	Aerotaxis receptor	0.08
PMI0182	NA	Transcriptional regulator	0.07
PMI1667	*cheW*	Purine-binding chemotaxis protein	0.07
PMI1657	*flgN*	Flagellar synthesis protein	0.06
PMI1656	*flgM*	Anti-σ^{28} factor FlgM	0.06
PMI1664	*cheR*	Chemotaxis methyltransferase CheR	0.05
PMI1645	*flgK*	Flagellar hook-associated protein 1	0.05
PMI1668	*cheA*	Chemotaxis protein CheA	0.04
PMI1665	NA	Methyl-accepting chemotaxis protein	0.03
PMI1669	*motB*	Chemotaxis protein (motility protein B)	0.02
PMI1666	NA	Methyl-accepting chemotaxis protein	0.02
PMI1670	*motA*	Flagellar motor protein MotA	0.02
PMI1621	*fliD*	Flagellar capping protein	0.01
PMI1620	*flaA*	Flagellin 1	0.01

[a] NA, not applicable; ACP, acyl carrier protein; MFS, major facilitator superfamily.

pared to that of wild-type swimmer cells, 122 genes were found to be differentially expressed (Table 3). Genes for propanediol utilization and microcompartment proteins (PMI2716 to PMI2722) were among the most highly induced genes in pseudoswarmer cells (see Table S3 in the supplemental material), an unexpected result, as none of these genes have been previously associated with

swarmer cell differentiation. While their role in swarming is uncertain, expression of these genes is indicative of 1,2-propanediol degradation, which may then provide a source of ATP as well as important three-carbon nutrients. GoMiner analysis identified significant decreases in transcription in genes associated with flagellar organization ($P = 2.8 \times 10^{-7}$), motility ($P = 2.5 \times 10^{-9}$),

TABLE 4 Expression levels of genes shared between wild-type swarmer cells and *fliL* pseudoswarmer cells

Locus tag	Gene[a]	Fold change in:	
		Swarmer cells	*fliL* cells
PMI1647	*flgI*	30.94	2.97
PMI1650	*flgF*	101.75	2.90
PMI1710	NA	4.08	2.80
PMI1720	NA	5.39	3.43
PMI1721	NA	6.34	3.70
PMI1722	NA	23.58	5.42
PMI2662	NA	0.01	0.35

[a] NA, not applicable.

and chemotaxis ($P = 1.8 \times 10^{-9}$) (Fig. 1), underscoring the motility defects observed in BB2204. While flagellar-gene expression decreased, fimbrial-gene expression increased in *fliL* pseudoswarmer cells (Table 3; Fig. 1), demonstrating a reciprocal control of flagellar and fimbrial biosynthesis, as previously observed (36).

Seven genes shared similar patterns of regulation in both *fliL* pseudoswarmer and wild-type swarmer cell transcriptomes. Expression of *flgI* and *flgF*, along with PMI1710, PMI1720, PMI1721, and PMI1722, encoding putative phage proteins, increased in both cell types, while the expression of PMI2662 (encoding a chitin-binding protein) decreased (Table 4). Analysis of the genetic neighborhood surrounding the prophage genes (43) revealed that this locus is immediately adjacent to the *rcs* locus, PMI1729 to PMI1731.

A direct comparison of the *fliL* pseudoswarmer transcriptome to that of the wild-type swarmer cell showed that, in addition to decreased expression in genes required for biosynthesis of the flagellum, pseudoswarmer cells also had decreased expression of *flhD* and *flhC* (approximately 8-fold and 11-fold, respectively) compared to wild-type swarmer cells (Table 5). Repression of genes encoding putative transcriptional regulatory proteins was also observed in pseudoswarmer cells (see Table S4 in the supplemental material), including that of *umoA*, whose expression has been shown to be positively correlated with that of *flhDC* (20).

The expression of *flhD*, *motA*, *flaA*, *umoA*, *zapA*, and *hpmB* was measured by quantitative RT-PCR (qRT-PCR) to verify the results of the RNA-Seq data. Statistical analyses indicate a high degree of correlation between the qRT-PCR and RNA-Seq data sets with both mRNA and total RNA (Fig. 2) as templates. Thus, the RNA-Seq data provide an accurate reflection of changes in gene expression.

Identification and characterization of *fliL* motile revertants. In parallel with transcriptomic analyses, we examined a set of 21 motile revertants that spontaneously arose from BB2204. Of these revertants, 81% (17 of the 21) were sensitive to chloramphenicol (Cm), indicating that the mutation was in or near the transposon inserted in *fliL*. Sixteen of 17 (94%) of the Cm-sensitive revertants had the same phenotype and possessed wild-type motility. Therefore, one of the 16 motile revertants, called YL1001, was chosen for further analyses.

Unlike the parent (BB2204) cells, YL1001 cells swim and swarm at near-wild-type levels (Fig. 3A and B), yet YL1001 develops pseudoswarmer cells inappropriately in liquid media (Fig. 3C to E). YL1001 produced the greatest number of pseudoswarmer cells 2.5 to 3 h after inoculation (Fig. 3F and G), which is also the peak of pseudoswarmer cell production by BB2204 and is also very

TABLE 5 Expression of the 50 most highly differentially expressed genes in *fliL* pseudoswarmer cells versus wild-type swarmer cells

Locus tag	Gene[a]	Product	Fold change
PMI1406	*gadC*	Glutamate/gamma-aminobutyrate antiporter	83.36
PMI0781	*rmf*	Ribosome modulation factor	77.14
PMI1011	NA	Hypothetical protein	73.96
PMI1224	NA	ABC-type multidrug transport system	73.32
PMI0068	NA	Hypothetical protein	71.61
PMI2221	NA	Fimbrial outer membrane usher protein	67.24
PMI0033	*hybB*	Putative hydrogenase 2 b cytochrome subunit	60.58
PMI1804	NA	Ferritin-like protein	53.81
PMI2662	NA	Chitin binding protein	52.25
PMI3209	*emrD*	Multidrug resistance protein D	49.74
PMI0069	NA	Putative oxidoreductase	47.71
PMI1225	NA	ABC-2 type transporter	45.85
PMI1395	NA	Hypothetical protein	43.30
PMI1223	NA	HlyD-family secretion protein	43.30
PMI1816	*phsC*	Thiosulfate reductase cytochrome b subunit	43.29
PMI0031	*hyb0*	Hydrogenase 2 small subunit	39.18
PMI1814	*phsA*	Thiosulfate reductase precursor	34.93
PMI0035	*hybD*	Hydrogenase 2 maturation protease	34.83
PMI3001	NA	Fimbrial protein	34.25
PMI1878	*pmfC*	Outer membrane usher protein	29.81
PMI0223	NA	Alpha-keto acid decarboxylase	28.42
PMI1532	NA	Glucose 1-dehydrogenase	26.85
PMI0032	*hybA*	Hydrogenase 2	26.61
PMI2763	*aceA*	Isocitrate lyase	24.67
PMI1668	*cheA*	Chemotaxis protein	0.01
PMI1628	NA	Metalloelastase	0.01
PMI1635	*fliK*	Flagellar hook-length control protein	0.01
PMI1665	NA	Methyl-accepting chemotaxis protein	0.01
PMI1650	*flgF*	Flagellar basal-body rod protein	0.01
PMI1632	*fliH*	Flagellar assembly protein H	0.01
PMI1670	*motA*	Flagellar motor protein	0.01
PMI1652	*flgD*	Basal-body rod modification protein	0.01
PMI2808	NA	Methyl-accepting chemotaxis protein	0.01
PMI1634	*fliJ*	Flagellar biosynthesis chaperone	0.01
PMI1644	*flgL*	Flagellar hook-associated protein 3 (hook-filament junction)	0.01
PMI1649	*flgG*	Flagellar basal-body rod protein (distal rod protein)	0.01
PMI1638	*fliN*	Flagellar motor switch protein	0.01
PMI1669	*motB*	Motility protein B	0.01
PMI1631	*fliG*	Flagellar motor switch protein G	0.01
PMI1630	*fliF*	Flagellar MS-ring protein	0.01
PMI1654	*flgB*	Flagellar basal body rod protein	0.01
PMI1651	*flgE*	Flagellar hook protein FlgE	0.01
PMI1637	*fliM*	Flagellar motor switch protein	0.00
PMI1666	NA	Methyl-accepting chemotaxis protein	0.00
PMI1629	*fliE*	Flagellar hook-basal body complex protein	0.00
PMI1645	*flgK*	Flagellar hook-associated protein 1	0.00
PMI1618	*fliA*	Flagellar biosynthesis sigma factor	0.00
PMI1653	*flgC*	Flagellar basal-body rod protein	0.00
PMI1621	*fliD*	Flagellar capping protein	0.00
PMI1620	*flaA*	Flagellin 1	0.00

[a] NA, not applicable.

similar to the time required for wild-type swarming to occur on agar. As has been previously reported for BB2204 (16), only a small percentage of the total population of YL1001 formed pseudoswarmer cells, suggesting that *fliL* defects may be bistable and that the surface-sensing pathway is complex, with multiple inputs that ultimately lead to swarmer cell differentiation.
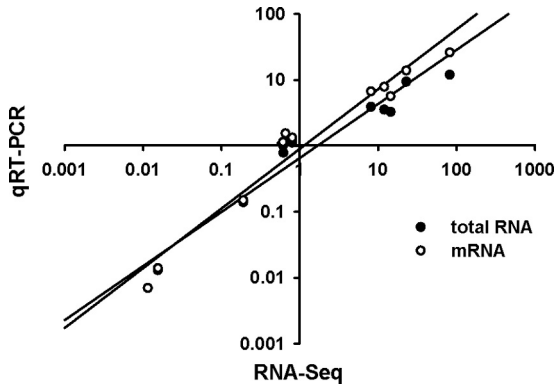
FIG 2 Verification of RNA-Seq gene expression analysis by qRT-PCR. Individual gene expression ratios were calculated using RPKM values generated via RNA-Seq and plotted against calculations done for the same gene using qRT-PCR on both total RNA and mRNA as templates. Each qRT-PCR assay was performed on the sample subject to RNA-Seq plus two independent samples. Pearson correlations of 0.964 ($P = 5.5 \times 10^{-7}$) and 0.898 ($P = 7.5 \times 10^{-5}$) were obtained when mRNA and total RNA served as the template, respectively, in the qRT-PCRs.

Previous reports (16) have shown that the transposon insertion in *fliL* of BB2204 (*fliL$_{2204}$*) is located at nucleotide 440, which is 44 bp from the stop codon in the 483-bp gene. Analysis of the sequence of YL1001 *fliL* (*fliL$_{1001}$*) revealed that the transposon had partially excised from its initial insertion site, leaving a 68-bp scar, as shown in Fig. 4A. Excision of the transposon restored transcription to the genes downstream of *fliL* in this operon, as well as to class III genes, e.g., *flaA* (flagellin), and provides an explanation for the motility of the revertants.

Closer examination of the *fliL$_{2204}$* sequence revealed a frameshift near the 3′ end of the gene, such that the C-terminal 14 amino acids of FliL$_{2204}$ were replaced with a portion of Tn5 sequence. As shown in Fig. 5, this changed the C terminus by adding 10 new amino acids, including multiple arginine and proline residues. A similar, but not identical, change also occurred in the C terminus of FliL$_{1001}$, resulting in an additional 28 residues at its C terminus (Fig. 5). This alteration of the C terminus of FliL may be responsible for the pseudoswarmer cell phenotype and suggests that the C-terminal domain of FliL is functionally important.

Expression of FlhD$_4$C$_2$, the flagellar master regulator, increases during swarmer cell development and swarming (24), and, as shown in Table S2, the current RNA-Seq measurements show that transcription of both *flhD* and *flhC* increased ca. 12- and 8-fold (respectively) in the swarmer transcriptome. With these results in mind, we measured the expression of *flhDC*, flagellar class II and III genes regulated by FlhD$_4$C$_2$, and the *umo* transcriptional regulators using qRT-PCR, to compare their expression in BB2204 and YL1001 pseudoswarmer cells relative to BB2000 swimmer cells. As can be seen in Fig. 6A, *flhD* was minimally induced in pseudoswarmer cells, while *flhD* expression increased 1.37-fold in BB2204 and 1.74-fold in YL1001. Unlike *flhD* expression, expression of flagellar class II genes, e.g., *fliA* and *fliL*, increased to moderate to high levels in pseudoswarmer cells of both BB2204 (20.42-fold increase in *fliA* and 6.11-fold increase in *fliL*) and YL1001 (4.38-fold increase in *fliA* and 3.59-fold increase in *fliL*). This result suggests that an increase in FlhD$_4$C$_2$ activity, rather than its transcription, occurs in pseudoswarmer cells. The increased *fliA* transcription in BB2204 may be due to a lack of feedback from
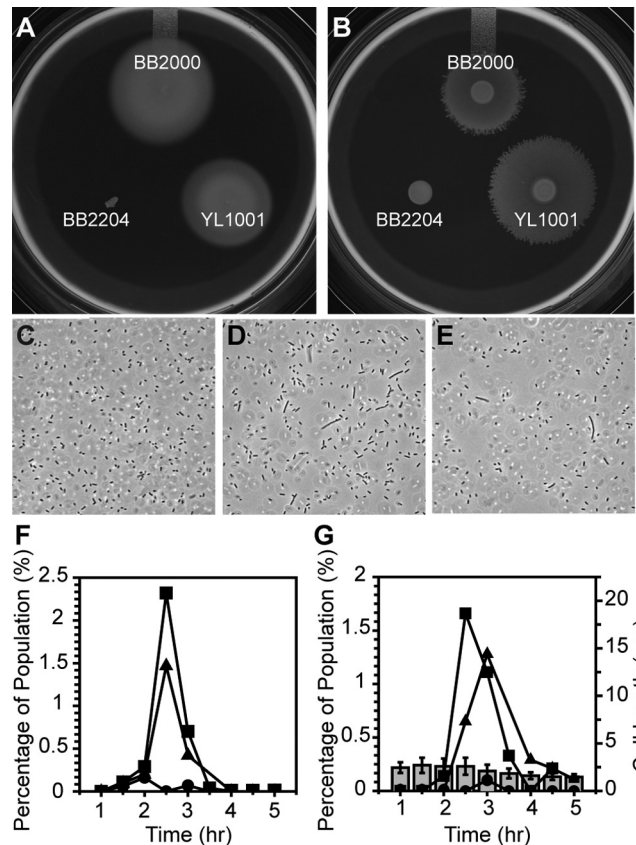
FIG 3 Swimming, swarming, and cellular elongation of wild-type and pseudoswarmer cells. Swimming (A) was measured using semisolid Mot agar, and swarming (B) was measured on LB agar. (C to E) Phase-contrast micrographs of BB2000 (C), BB2204 (D), and YL1001 (E) taken after growth in LB broth. (F and G) Determination of the percent elongated cells in the populations of BB2000 (●), BB2204 (■), and YL1001 (▲). (F) Percentage of cells with a length of >7 μm; (G) percentage of cells with a length >3-fold greater than the floating standard (see Materials and Methods). Error bars represent standard deviations ($n > 400$).

flagellar class III gene products, rather than defects in *fliL*, as can be seen by the high levels of repression of both *flgM* and *flaA* transcripts (Fig. 6A). As shown in Fig. 6B, defects in *fliL* increase *umoA* expression in BB2204 pseudoswarmer cells more than 6-fold but result in only a minimal increase (1.59-fold) in the expression of *umoA* in YL1001 pseudoswarmer cells. The increase in *umoA* expression in BB2204 pseudoswarmer cells was unexpected, since expression of *umoA* did not change according to RNA-Seq analysis; however, this discrepancy is likely due to the different times at which cells were harvested (4.5 h for RNA-Seq analysis for comparison with wild-type swarmer cells versus 2.5 h for comparison with YL1001 *fliL* pseudoswarmers). No changes in expression in *umoB*, *umoC*, or *umoD* were observed in either BB2204 or YL1001 pseudoswarmer cells.

DISCUSSION

The connection between motile behavior, FliL, and regulation of the motile versus sessile mode of existence has emerged as a theme among bacteria, as first noted by Christen et al. (18) and recently reviewed by Wolfe and Visick (58). Recent reports have provided evidence that the function of FliL is to support the inherently weak
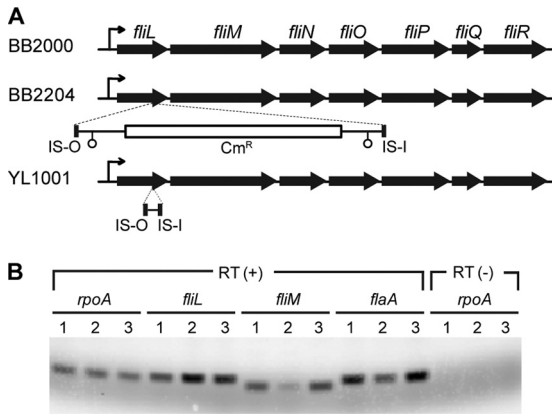
FIG 4 Expression of *fliL* operon genes and *flaA* in pseudoswarmer cells. (A) Organization of the *fliL* operon in BB2000, BB2204, and YL1001. Mini-Tn*5*-Cm^r (~2 kb) disrupts *fliL*$_{2204}$ at nucleotide 440, and *fliL*$_{YL1001}$ is mutated by a 68-bp scar following excision of the transposon. The *fliL* promoter is indicated by a bent arrow, and open circles represent transcriptional terminators in the mini-Tn*5* transposon. (B) RT-PCR analysis of transcription of class II (*fliL* and *fliM*) and class III (*flaA*) flagellar genes, relative to *rpoA* (as a positive referential control). Lanes: 1, BB2000; 2, BB2204; 3, YL1001. RT(+) indicates complete reverse transcriptase PCR, while RT(−) lanes lack reverse transcriptase and serve as a control for DNA contamination.

joint between the proximal and distal rod proteins. When *P. mirabilis* swimmer cells encounter a surface, the rotation of their flagella is inhibited, triggering differentiation into a swarmer cell with renewed flagellar motility. How do the bacteria sense the surface? In the current study, we used transcriptomic and genetic methods to understand the molecular mechanism underlying this signal transduction circuit.

The increased expression of *umoA* in swarmer cells (23-fold increase) and pseudoswarmer cells (ca. 6.2-fold) (Fig. 6B; also, see Table S2 in the supplemental material) is an exciting discovery that potentially links FliL function to a known regulator of swarmer cell differentiation (20). Dufour et al. (20) reported that UmoA resides in the outer membrane and its activity is negatively regulated by flagellar class II genes. Therefore, the increases in *umoA* expression observed here may be due to an indirect effect caused by the *fliL* mutations in the pseudoswarmer strains used in our study. Indeed, transcription of *umoA* is dependent upon other factors, and one of these is proper flagellar assembly. This can be seen by comparing *umoA* transcription in nonmotile *fliL* mutants (6.2-fold increase in *umoA*) with that of swimming *fliL* revertants,

such as YL1001 (1.6-fold increase in *umoA*) (Fig. 6B). However, negative regulation by class II genes does not explain the increased *umoA* expression in wild-type swarmer cells (that have intact *fliL*), unless *umoA* expression depends on a functional FliL protein. In such a scenario, one may imagine that inhibition of flagellar rotation occurs when a swimmer cell is placed on a surface, resulting in increased torque on FliL. Torsional forces may lead to conformational changes in FliL that adversely affect its function and ultimately result in an increase in *umoA* expression. This likely occurs through FliL protein-protein interactions. In support of this hypothesis, Li and Sourjik recently showed using FRET measurements that *E. coli* FliL interacts strongly with itself and weakly with FliG (35). Suaste-Olmos et al. (53) identified single-base-pair changes in *motB* in a search for *fliL* suppressor mutations of *Rhodobacter sphaeroides* (29) and supported by reports demonstrating a direct interaction between FliL and MotB in *Campylobacter jejuni* (46). Experiments are under way in our laboratory to measure FliL protein-protein interactions and determine their function in surface signaling and swarmer cell differentiation.

What domains of FliL are important to its function? Our data indicate that the C-terminal domain of *P. mirabilis* FliL is required for full activity. The FliL mutants examined in this study each have the C-terminal 14 amino acids of the protein, QILSDVLFTTFILR, replaced with residues derived from mini-Tn*5* (Fig. 5). Twenty-four new amino acids replace the original 14 residues of FliL$_{2204}$, increasing the length of the protein and its charge. In FliL$_{1001}$, 42 amino acids replace the original 14, bringing at least 8 charged residues (7 arginines and a lysine) not found in wild-type FliL. Since FliL has a single transmembrane domain close to the N terminus, the changes observed in the C terminus of FliL are unlikely to affect the localization of protein. Furthermore, loss of the C-terminal 15 amino acids from *R. sphaeroides* FliL does not affect interaction with itself (53), suggesting that the changes in FliL$_{2204}$ and FliL$_{1001}$ we observed affect how FliL interacts with other, currently unknown proteins.

Undoubtedly, due to its location in the periplasm and lack of amino acid domains indicative of a transcriptional regulator, FliL acts as an intermediate processor in the surface signal transduction pathway, relaying information to FlhD$_4$C$_2$. As shown in Table S2 in the supplemental material, expression of *flhDC* increases during swarmer cell differentiation (24), but our results also indicate that FlhD$_4$C$_2$ activity is affected when *fliL* is mutated, specifically in BB2204 pseudoswarmer cells (Fig. 6A). Increased FlhD$_4$C$_2$ activity is evident from the significant elevation in tran-
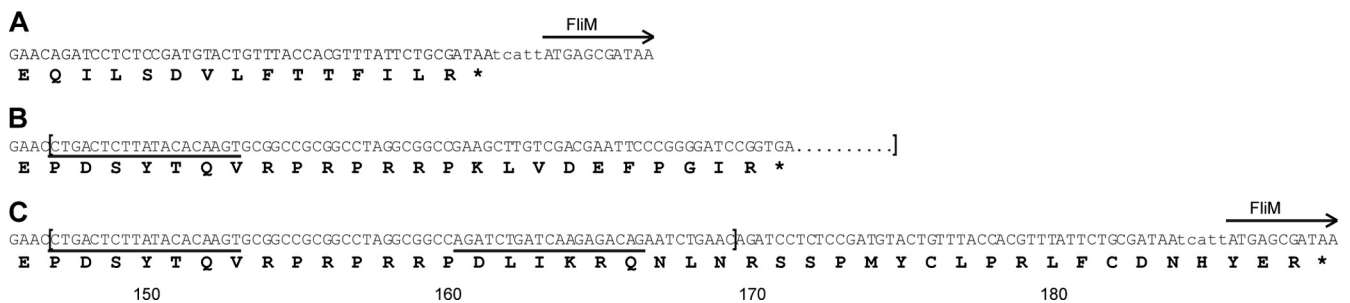
FIG 5 Characterization of the *fliL* mutations resulting in the pseudoswarmer phenotype. Nucleotide (top) and deduced amino acid (bottom) sequences of the C terminus of FliL of BB2000 (A), BB2204 (B), and YL1001 (C) are shown. Brackets indicate the mini-Tn*5*-Cm^r sequence, and underlining indicates IS elements of the transposon.
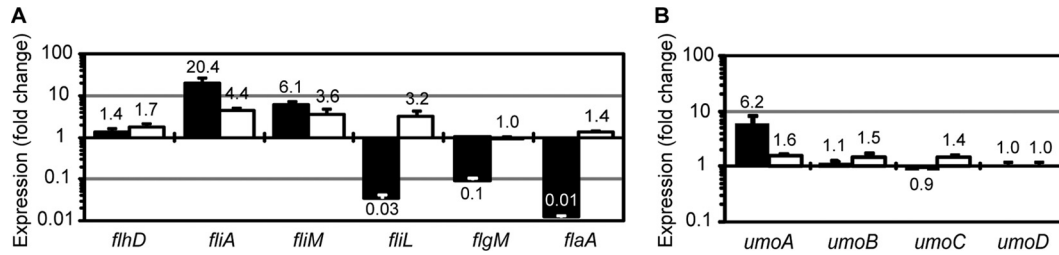
FIG 6 Transcription of hallmark genes in *fliL* pseudoswarmer strains. (A) Expression of the *flhD* gene (class I), the *fliL*, *fliM*, and *fliA* genes (all class II), and the *flgM* and *flaA* genes (both class III). (B) Expression of *umoA* to *umoD* genes. Filled bars, BB2204; open bars, YL1001. Expression in each pseudoswarmer strain was compared with the expression of the same gene in wild-type swimmer cells. A >1 change indicates that expression of the gene is greater in the pseudoswarmer cells than in swimmer cells, while a value of <1 means that expression decreases in the pseudoswarmer strain. Error bars indicate standard errors for three independent measurements from three biological samples.

scription of the class II operons, *fliA* and *fliL*, without a concomitant change in expression of *flhD* (Fig. 6A). Regulation of flagellar gene expression is a hierarchical process governed by the state of flagellum biosynthesis, with checkpoints to coordinate transcription with proper assembly, and feedback occurs between class II and class III gene products and FlhD$_4$C$_2$ activity (2, 24). For example, FliD and FliT (class III operon genes) inhibit FlhD$_4$C$_2$ activity, while FliZ (within the class II *fliA* operon) positively affects *flhDC* (2, 48, 49, 59). The Tn5 insertion in *fliL$_{2204}$* prevents expression of the genes downstream of *fliL* that encode components of the flagellar basal body and export apparatus, and this results in a loss of class III gene expression (i.e., *flaA* expression [Fig. 6A]). We hypothesize that this in turn produces a negative feedback effect on FlhD$_4$C$_2$ activity.

One of the hallmarks of swarmer cell differentiation is the large increase in flagella per cell, which is readily seen by the number of flagellum-associated genes whose expression increased in the swarmer cell transcriptome (Table 2; Fig. 1; also, see Table S2 in the supplemental material) and decreased in the transcriptome of nonmotile BB2204 pseudoswarmer cells (Fig. 1 and 6A; Table 3). However, not all flagellar gene expression decreased in pseudoswarmer transcriptomes, as both *flgI* (P ring) and *flgF* (proximal rod protein) expression increased (Table 3). We believe that the increase in *flgF* expression is significant, since FlgF is physically adjacent to FlgG, the distal rod protein, in the basal body, and hypothesize that an increase in *flgF* (and perhaps *flgI*) expression may be a means used by pseudoswarmer cells to compensate for the loss of FliL. This hypothesis is currently being tested in our laboratory. It is noteworthy that RNA-Seq analysis further supports this hypothesis through the identification of three additional rod-associated genes whose expression increased in pseudoswarmer cells. These include *flgD*, whose product is a basal-body rod modification protein (5-fold increase in expression), and *flgB* (2.63-fold increase in expression) and *flgC* (1.6-fold increase in expression), both encoding basal body rod proteins. While the change in expression of these three rod proteins did not pass our criteria for statistical significance (i.e., a change of >2-fold, with a *P* value of <0.05), the increased expression of these rod protein genes may hint at a possible mechanism by which cells compensate for loss of FliL.

Genes whose products are components of the outer surface of the bacterium or affect membrane fluidity and permeability (Table 2; also, see Table S2 in the supplemental material) also had marked changes in expression resulting from swarmer cell differentiation. Swarmer cells had increased expression of multiple li-

poproteins, a glycoporin, outer membrane proteins of unknown function, a glycosyl hydrolase, and a β-phosphoglucomutase, all of which are indicative of a significant restructuring of the cell wall. These results complement previous reports documenting changes in capsular polysaccharide, lipopolysaccharide, and membrane composition as vegetative cells differentiate into swarmer cells (8–10, 14, 25, 27).

The deep-sequencing capability of RNA-Seq resulted in identification of genes not previously associated with swarmer cell differentiation and, of these, those located within a degenerate prophage region (43). Overall, half the genes in this region were induced in swarmer cells, while one-third were induced in *fliL* pseudoswarmers (see Tables S2 and S3 in the supplemental material). We do not fully understand why the expression of these prophage genes increases in conjunction with swarmer cell differentiation; however, it is worth noting that they lie adjacent to three genes—*rcsD* (formerly *rsbA*), *rcsB*, and *rcsC*—that encode the Rcs regulatory circuit, which acts to inhibit swarmer cell differentiation and *flhDC* expression (15).

A second group of genes not previous associated with the differentiated swarmer cell are those encoding microcompartment proteins whose expression increased in *fliL* pseudoswarmer cells. Microcompartments are proteinaceous organelles that encapsulate the enzymes that participate in metabolic pathways, including B$_{12}$-dependent 1,2-propanediol degradation (17). Not only is the expression of genes encoding microcompartment proteins elevated in a *fliL* background, but the expression of propanediol utilization proteins and aldehyde-alcohol dehydrogenase also increases (Table 3). These processes may aid *P. mirabilis* by providing increased ATP and an electron sink, as well as important three-carbon nutrients, and have been shown to alleviate DNA and cellular damage in other species (51). We hypothesize that defects in FliL may cause stress or damage to the bacteria, and the elevated expression of the microcompartment proteins reflects the cell's attempts to limit the damage from the mutation.

Many of the results from the current analysis corroborate earlier reports of the *P. mirabilis* swarmer cell transcriptome (42). The genes in common include those involved with flagellar motility, assembly, and organization; chemotaxis; amino acid biosynthesis (*cysP*, *cysD*); outer membrane modification and transport proteins (*exbD*, *exbB*, PMI1359, PMI0842); and the regulatory proteins Ccm and PMI0182. However, there are a few notable differences between the present and previous studies, particularly in the expression of genes encoding lipoproteins and outer membrane proteins. While differences in culture conditions (30°C ver-

sus 37°C), strains (HI4320 versus BB2000) and method of measurement (microarray versus RNA-Seq) likely contributed to differences between the two data sets, we believe that the discrepancies are primarily due to differences in the time at which swarmer cells were harvested (overnight versus 4.5 h) and reflect transient and short-lived expression of genes during the dynamic process of swarmer cell differentiation. Indeed, we did not observe significant changes in either *zapA* or *hpmB*, whose expression we previously observed to be correlated with swarming (4, 56) and increased in a *fliL* background (16). The expression of *zapA* is greatest immediately before the consolidation phase of swarming (5.5 h). In the current study, swarmer cells were harvested from nutrient agar at 4.5 h, when maximal swarming motility is observed, while pseudoswarmer cells were harvested after 2.5 h of incubation in nutrient broth, when the highest numbers of elongated cells were present. Therefore, the lack of *zapA* expression is likely due to the time at which the cells were harvested and reflects the rise and fall in *zapA* expression during swarming colony migration (56).

Collectively, our results shed new light on the cellular components involved in the surface signaling pathway of *P. mirabilis* and indicate that FliL plays a key role in transducing the signal, via its C-terminal domain. It remains unknown how FliL transmits the information from the stalled flagellar motor to FlhD$_4$C$_2$, but we hypothesize that UmoA is part of this pathway. Experiments are in progress to investigate this possibility.

ACKNOWLEDGMENTS

REFERENCES

1. **Alavi M, Belas R.** 2001. Surface sensing, swarmer cell differentiation, and biofilm development. Methods Enzymol. **336**:29–40.
2. **Aldridge C, et al.** 2010. The interaction dynamics of a negative feedback loop regulates flagellar number in *Salmonella enterica* serovar Typhimurium. Mol. Microbiol. **78**:1416–1430.
3. **Allison C, Coleman N, Jones PL, Hughes C.** 1992. Ability of *Proteus mirabilis* to invade human urothelial cells is coupled to motility and swarming differentiation. Infect. Immun. **60**:4740–4746.
4. **Allison C, Lai HC, Hughes C.** 1992. Coordinate expression of virulence genes during swarm cell differentiation and population migration of *Proteus mirabilis*. Mol. Microbiol. **6**:1583–1591.
5. **Anders S, Huber W.** 2010. Differential expression analysis for sequence count data. Genome Biol. **11**:R106.
6. **Arakawa K, Kono N, Yamada Y, Mori H, Tomita M.** 2005. KEGG-based pathway visualization tool for complex omics data. In Silico Biol. **5**:419–423.
7. **Arezi B, Xing W, Sorge JA, Hogrefe HH.** 2003. Amplification efficiency of thermostable DNA polymerases. Anal. Biochem. **321**:226–235.
8. **Armitage JP.** 1982. Changes in the organisation of the outer membrane of *Proteus mirabilis* during swarming: freeze-fracture structure and membrane fluidity analysis. J. Bacteriol. **150**:900–904.
9. **Armitage JP, Rowbury RJ, Smith DG.** 1975. Indirect evidence for cell wall and membrane differences between filamentous swarming cells and short non-swarming cells of *Proteus mirabilis*. J. Gen. Microbiol. **89**:199–202.
10. **Armitage JP, Smith DG, Rowbury RJ.** 1979. Alterations in the cell envelope composition of *Proteus mirabilis* during the development of swarmer cells. Biochim. Biophys. Acta **584**:389–397.
11. **Attmannspacher U, Scharf BE, Harshey RM.** 2008. FliL is essential for swarming: motor rotation in absence of FliL fractures the flagellar rod in swarmer cells of *Salmonella enterica*. Mol. Microbiol. **68**:328–341.
12. **Belas R.** 1994. Expression of multiple flagellin-encoding genes of *Proteus mirabilis*. J. Bacteriol. **176**:7169–7181.
13. **Belas R, Erskine D, Flaherty D.** 1991. Transposon mutagenesis in *Proteus mirabilis*. J. Bacteriol. **173**:6289–6293.
14. **Belas R, Goldman M, Ashliman K.** 1995. Genetic analysis of *Proteus mirabilis* mutants defective in swarmer cell elongation. J. Bacteriol. **177**:823–828.
15. **Belas R, Schneider R, Melch M.** 1998. Characterization of *Proteus mirabilis* precocious swarming mutants: identification of *rsbA*, encoding a regulator of swarming behavior. J. Bacteriol. **180**:6126–6139.
16. **Belas R, Suvanasuthi R.** 2005. The ability of *Proteus mirabilis* to sense surfaces and regulate virulence gene expression involves FliL, a flagellar basal body protein. J. Bacteriol. **187**:6789–6803.
17. **Cheng SQ, Liu Y, Crowley CS, Yeates TO, Bobik TA.** 2008. Bacterial microcompartments: their properties and paradoxes. Bioessays **30**:1084–1095.
18. **Christen M, et al.** 2007. DgrA is a member of a new family of cyclic diguanosine monophosphate receptors and controls flagellar motor function in *Caulobacter crescentus*. Proc. Natl. Acad. Sci. U. S. A. **104**:4112–4117.
19. **Coker C, Poore CA, Li X, Mobley HLT.** 2000. Pathogenesis of *Proteus mirabilis* urinary tract infection. Microbes Infect. **2**:1497–1505.
20. **Dufour A, Furness RB, Hughes C.** 1998. Novel genes that upregulate the *Proteus mirabilis flhDC* master operon controlling flagellar biogenesis and swarming. Mol. Microbiol. **29**:741–751.
21. **Edgar R, Domrachev M, Lash AE.** 2002. Gene Expression Omnibus: NCBI gene expression and hybridization array data repository. Nucleic Acids Res. **30**:207–210.
22. **Ferrieres L, Clarke DJ.** 2003. The RcsC sensor kinase is required for normal biofilm formation in *Escherichia coli* K-12 and controls the expression of a regulon in response to growth on a solid surface. Mol. Microbiol. **50**:1665–1682.
23. **Fraser GM, Hughes C.** 1999. Swarming motility. Curr. Opin. Microbiol. **2**:630–635.
24. **Furness RB, Fraser GM, Hay NA, Hughes C.** 1997. Negative feedback from a *Proteus* class II flagellum export defect to the *flhDC* master operon controlling cell division and flagellum assembly. J. Bacteriol. **179**:5585–5588.
25. **Gué M, Dupont V, Dufour A, Sire O.** 2001. Bacterial swarming: a biochemical time-resolved FTIR-ATR study of *Proteus mirabilis* swarm-cell differentiation. Biochemistry **40**:11938–11945.
26. **Gygi D, Bailey MJ, Allison C, Hughes C.** 1995. Requirement for FlhA in flagella assembly and swarm cell differentiation by *Proteus mirabilis*. Mol. Microbiol. **15**:761–769.
27. **Gygi D, et al.** 1995. A cell-surface polysaccharide that facilitates rapid population migration by differentiated swarm cells of *Proteus mirabilis*. Mol. Microbiol. **17**:1167–1175.
28. **Harle C, Kim I, Angerer A, Braun V.** 1995. Signal transfer through three compartments: transcription initiation of the *Escherichia coli* ferric citrate transport system from the cell surface. EMBO J. **14**:1430–1438.
29. **Hosking ER, Vogt C, Bakker EP, Manson MD.** 2006. The *Escherichia coli* MotAB proton channel unplugged. J. Mol. Biol. **364**:921–937.
30. **Jacobsen SM, Stickler DJ, Mobley HLT, Shirtliff ME.** 2008. Complicated catheter-associated urinary tract infections due to *Escherichia coli* and *Proteus mirabilis*. Clin. Microbiol. Rev. **21**:26–59.
31. **Kearns DB.** 2010. A field guide to bacterial swarming motility. Nat. Rev. Microbiol. **8**:634–644.
32. **Komeda Y.** 1982. Fusions of flagellar operons to lactose genes on a mu lac bacteriophage. J. Bacteriol. **150**:16–26.
33. **Kutsukake K, Ohya Y, Iino T.** 1990. Transcriptional analysis of the flagellar regulon of *Salmonella typhimurium*. J. Bacteriol. **172**:741–747.
34. **Li H, Durbin R.** 2009. Fast and accurate short read alignment with Burrows-Wheeler transform. Bioinformatics **25**:1754–1760.
35. **Li H, Sourjik V.** 2011. Assembly and stability of flagellar motor in *Escherichia coli*. Mol. Microbiol. **80**:886–899.
36. **Li X, Rasko DA, Lockatell CV, Johnson DE, Mobley HLT.** 2001.

Repression of bacterial motility by a novel fimbrial gene product. EMBO J. **20**:4854–4862.

37. **Livak KJ, Schmittgen TD.** 2001. Analysis of relative gene expression data using real-time quantitative PCR and the $2^{-\Delta\Delta CT}$ method. Methods **25**:402–408.

38. **Macnab RM.** 1996. Flagella and motility, p. 123–145. *In* Neidhardt FC eet al. (ed), *Escherichia coli* and *Salmonella*: cellular and molecular biology. ASM Press, Washington, DC.

39. **Morgenstein RM, Szostek B, Rather PN.** 2010. Regulation of gene expression during swarmer cell differentiation in *Proteus mirabilis*. FEMS Microbiol. Rev. **34**:753–763.

40. **Mortazavi A, Williams BA, McCue K, Schaeffer L, Wold B.** 2008. Mapping and quantifying mammalian transcriptomes by RNA-Seq. Nat. Methods **5**:621–628.

41. **Pearson MM, Mobley HLT.** 2008. Repression of motility during fimbrial expression: identification of 14 *mrpJ* gene paralogues in *Proteus mirabilis*. Mol. Microbiol. **69**:548–558.

42. **Pearson MM, Rasko DA, Smith SN, Mobley HLT.** 2010. Transcriptome of swarming *Proteus mirabilis*. Infect. Immun. **78**:2834–2845.

43. **Pearson MM, et al.** 2008. Complete genome sequence of uropathogenic *Proteus mirabilis*, a master of both adherence and motility. J. Bacteriol. **190**:4027–4037.

44. **Pfaffl MW.** 2001. A new mathematical model for relative quantification in real-time RT-PCR. Nucleic Acids Res. **29**:e45.

45. **Raha M, Sockett H, Macnab RM.** 1994. Characterization of the FliL gene in the flagellar regulon of *Escherichia coli* and *Salmonella typhimurium*. J. Bacteriol. **176**:2308–2311.

46. **Rajagopala SV, et al.** 2007. The protein network of bacterial motility. Mol. Syst. Biol. **3**:128.

47. **Rauprich O, et al.** 1996. Periodic phenomena in *Proteus mirabilis* swarm colony development. J. Bacteriol. **178**:6525–6538.

48. **Saini S, Brown JD, Aldridge PD, Rao CV.** 2008. FliZ Is a posttranslational activator of FlhD$_4$C$_2$-dependent flagellar gene expression. J. Bacteriol. **190**:4979–4988.

49. **Saini S, et al.** 2010. FliZ induces a kinetic switch in flagellar gene expression. J. Bacteriol. **192**:6477–6481.

50. **Sambrook J, Fritsch EF, Maniatis T.** 1989. Molecular cloning: a laboratory manual, 2nd ed. Cold Spring Harbor Laboratory Press, Cold Spring Harbor, NY.

51. **Sampson EM, Bobik TA.** 2008. Microcompartments for B$_{12}$-dependent 1,2-propanediol degradation provide protection from DNA and cellular damage by a reactive metabolic intermediate. J. Bacteriol. **190**:2966–2971.

52. **Sturgill G, Rather PN.** 2004. Evidence that putrescine acts as an extracellular signal required for swarming in *Proteus mirabilis*. Mol. Microbiol. **51**:437–446.

53. **Suaste-Olmos F, et al.** 2010. The flagellar protein FliL is essential for swimming in *Rhodobacter sphaeroides*. J. Bacteriol. **192**:6230–6239.

54. **Trapnell C, Pachter L, Salzberg SL.** 2009. TopHat: discovering splice junctions with RNA-Seq. Bioinformatics **25**:1105–1111.

55. **Trapnell C, et al.** 2010. Transcript assembly and quantification by RNA-Seq reveals unannotated transcripts and isoform switching during cell differentiation. Nat. Biotechnol. **28**:511–515.

56. **Walker KE, Moghaddame-Jafari S, Lockatell CV, Johnson D, Belas R.** 1999. ZapA, the IgA-degrading metalloprotease of *Proteus mirabilis*, is a virulence factor expressed specifically in swarmer cells. Mol. Microbiol. **32**:825–836.

57. **Wang Q, Frye JG, McClelland M, Harshey RM.** 2004. Gene expression patterns during swarming in *Salmonella typhimurium*: genes specific to surface growth and putative new motility and pathogenicity genes. Mol. Microbiol. **52**:169–187.

58. **Wolfe AJ, Visick KL.** 2008. Get the message out: cyclic-di-GMP regulates multiple levels of flagellum-based motility. J. Bacteriol. **190**:463–475.

59. **Yamamoto S, Kutsukake K.** 2006. FliT acts as an anti-FlhD$_2$C$_2$ factor in the transcriptional control of the flagellar regulon in *Salmonella enterica* serovar Typhimurium. J. Bacteriol. **188**:6703–6708.

60. **Zeeberg BR, et al.** 2003. GoMiner: a resource for biological interpretation of genomic and proteomic data. Genome Biol. **4**:R28.

61. **Zeeberg BR, et al.** 2005. High-throughput GoMiner, an 'industrial-strength' integrative gene ontology tool for interpretation of multiple-microarray experiments, with application to studies of common variable immune deficiency (CVID). BMC Bioinformatics **6**:168.